A Spectroscopic Study of Hexadecylquinolinium Tricyanoquinodimethanide as a Monolayer and in Bulk

ARTICLE *in* THE JOURNAL OF PHYSICAL CHEMISTRY B · SEPTEMBER 2002

Impact Factor: 3.3 · DOI: 10.1021/jp014486x

8 AUTHORS, INCLUDING:

Greg Szulczewski
University of Alabama
50 PUBLICATIONS **821** CITATIONS
SEE PROFILE

R R Amaresh
Makhteshim Agan India
16 PUBLICATIONS **332** CITATIONS
SEE PROFILE

Lowell D Kispert
University of Alabama
278 PUBLICATIONS **3,923** CITATIONS
SEE PROFILE

Robert Metzger
University of Alabama
201 PUBLICATIONS **6,665** CITATIONS
SEE PROFILE

A Spectroscopic Study of Hexadecylquinolinium Tricyanoquinodimethanide as a Monolayer and in Bulk

Tao Xu, Todd A. Morris, Greg J. Szulczewski,* Ramiya R. Amaresh, Yunlong Gao, Shane C. Street, Lowell D. Kispert, and Robert M. Metzger*

Department of Chemistry, The University of Alabama, Tuscaloosa, Alabama 35487-0336

Francesca Terenziani

Dipartimento di Chimica Generale ed Inorganica, Chimica Analitica e Chimica Fisica, INSTM-UdR Parma, Università degli Studî di Parma, Viale delle Scienze 17/A, I-43100 Parma, Italy

Received: December 10, 2001; In Final Form: July 16, 2002

We have prepared Langmuir−Blodgett monolayers of hexadecylquinolinium tricyanoquinodimethanide ($C_{16}H_{33}Q^+$-3CNQ$^-$) on gold surfaces and characterized the structure by surface plasmon resonance (SPR), X-ray photoelectron spectroscopy (XPS), reflection−absorption infrared spectroscopy (RAIRS), Raman spectroscopy, and water contact angle measurements. We compare the IR and UV−vis spectra of $C_{16}H_{33}Q^+$-3CNQ$^-$ to a series of compounds that contain the key functional groups in the titled compound to help assign the spectral features. The surface spectroscopic measurements indicate that the molecules in the monolayer are aligned such that the two terminal cyano groups are adsorbed on the Au surface, and that the aliphatic chain is away from that surface. The thickness of the monolayer was measured by XPS to be $\sim$ 26 Å and suggests that the molecules are tilted $\sim$40° away from the surface normal. High-resolution XPS and spectroelectrochemical measurements of $C_{16}H_{33}Q^+$-3CNQ$^-$ strongly suggest that it is a ground-state zwitterion in both the adsorbed and solvated forms.

Introduction

In the past five years, spectacular progress in the construction and measurement of molecular electronic devices has occurred. For example, molecular-based transistors[1] (although this result has not yet been confirmed independently), wires,[2] and rectifiers[3] have been demonstrated. We have demonstrated that a Langmuir−Blodgett (LB) monolayer of hexadecylquinolinium tricyanoquinodimethanide ($C_{16}H_{33}Q^+$-3CNQ$^-$) shows a rectifying current measured between two stationary macroscopic oxide-free gold electrodes,[4,5] provided that the molecular dipole moment is not perpendicular to the applied electric field.[3] Theoretical calculations of the current−voltage (I−V) characteristics of a single $C_{16}H_{33}Q^+$-3CNQ$^-$ molecule between gold electrodes show some agreement with the experimental data.[6] The molecular ground state was presumed to be a highly polar zwitterionic state $C_{16}H_{33}Q^+$-3CNQ$^-$, (Figure 1, structure **1**) that can be written schematically as $D^+-\pi-A^-$ (where D^+ is the hexadecylquinolinium moiety, π is the ethylene "bridge", and A^- is the tricyanoquinodimethanide moiety). Its first electronically excited state is presumably less polar, with structure $C_{16}H_{33}Q^0$-3CNQ^0.[7] The electrical asymmetry in the I−V characteristics was assigned to a favored direction of electron transfer within the molecule, from A^- to D^+[8].

Despite some previous work,[5,8,9] it is important to further investigate the orientation of the $C_{16}H_{33}Q^+$-3CNQ$^-$ molecules on a metal electrode, because theory predicts that the conductance of molecules is strongly dependent on orientation.[3,10−12] The film thickness of **1** as a monolayer on Au, Ag, and Al has been measured with a variety of techniques and ranges from 21 to 29 Å.[5,8,9] The discrepancy in these different values may be due to adventitious adsorbates, the nature of the substrate−monolayer interactions, and/or the intrinsic property that the method is measuring. These values, when compared to a theoretical estimate of the molecular length for the lowest-energy conformation, can yield the angle of tilt of the molecules relative to the surface normal.[8] The orientation and tilt of the molecules on the substrate, and the consequent orientation of the electrical dipole moment in both ground and excited states, should play a vital role in explaining the nature of the asymmetry in the current−voltage curves.[3,10] Consequently, the present study has two main objectives. First, to determine the thickness and orientation of $C_{16}H_{33}Q^+$-3CNQ$^-$ LB films on gold surfaces by several techniques. Second, to provide spectroscopic evidence for the highly polar zwitterionic form of the ground electronic state. To accomplish the first goal we used surface plasmon resonance (SPR), X-ray photoelectron spectroscopy (XPS), reflection−absorption infrared spectroscopy (RAIRS), Raman spectroscopy, and water contact angle measurements. To accomplish the second goal, we measured the steady-state absorption spectra[13,14] of the electrochemically oxidized or reduced form of $C_{16}H_{33}Q^+$-3CNQ$^-$.

Experimental Details

Preparation of the Bottom Gold Electrode. In a clean room, glass substrates (Corning 1747F) or Si (111) substrates (for XPS measurements) were cleaned by first rinsing with acetone for 2 min and then with 2-propanol for 2 min in an ultrasonic bath, followed by drying in a stream of dry nitrogen. Our evaporation chamber (Edwards E306) was pumped to a base pressure of 4 $\times$ 10^{-6} mbar using a liquid nitrogen trapped diffusion pump. A 5 nm Cr adhesion layer was first evaporated onto the glass or Si (111) substrate at the rate of 0.05 nm s^{-1}. Then, without

10.1021/jp014486x CCC: $22.00
Published on Web 09/18/2002

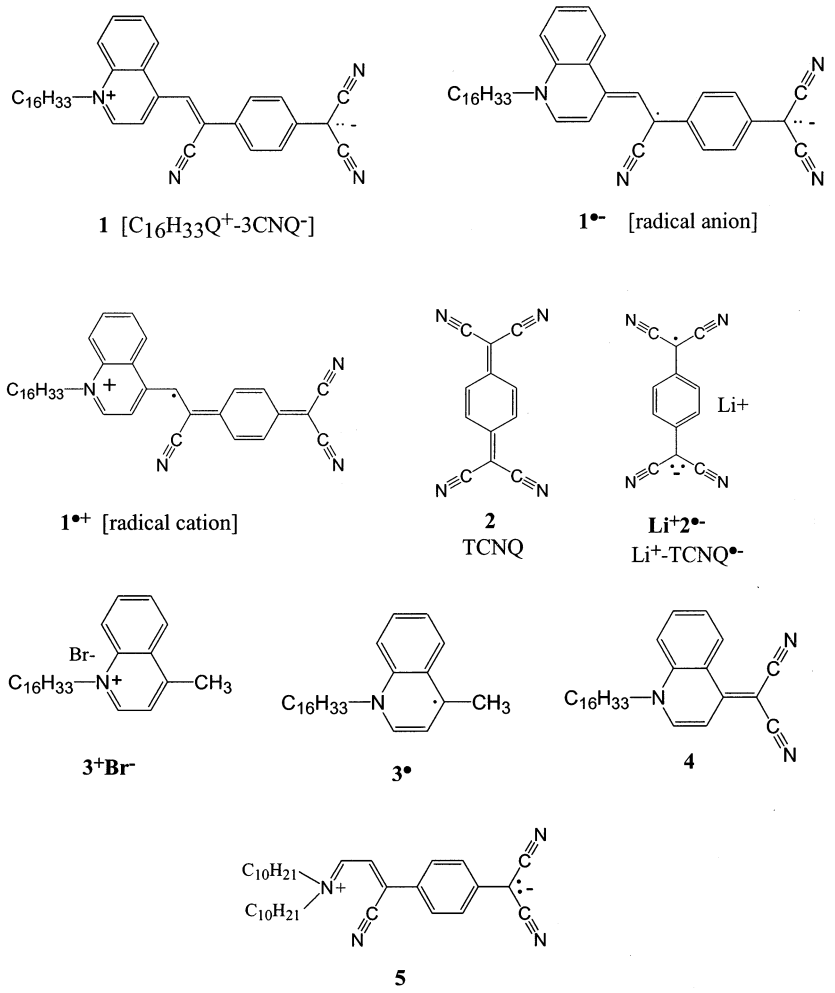

Figure 1. Structures of $C_{16}H_{33}Q^+$-3CNQ$^-$ (**1**) and related compounds.

breaking vacuum, 150 nm Au was evaporated atop the Cr from a Mo evaporator boat at 0.02 nm s^{-1}. The thickness of the films was measured with a quartz crystal thickness monitor.

LB−Film Deposition. The substrates were cleaned by UV/ozone (JeLight Co., Inc. model 42) for 80 s and immediately immersed into deionized pure water. The $C_{16}H_{33}Q^+$-3CNQ$^-$ was spread from dichloromethane onto pure water (Barnstead, 18.3 MΩ cm). At the air−water interface, a monolayer of $C_{16}H_{33}Q^+$-3CNQ$^-$ was transferred onto the Au film on the upstroke at 25 mN·m^{-1}. The transfer ratios were slightly greater than unity, presumably due to partial surface roughness. The samples were then desiccated in a vacuum over P_2O_5 for 72 h.

Surface Plasmon Resonance. SPR reflectivity curves were measured in the Kretchmann configuration[15] with a home-built apparatus. The output of a 15 mW polarized HeNe laser (632 nm) was attenuated to ∼1 mW. The beam was mechanically chopped (Stanford Research Systems, model 540) at 4 kHz, and passed through a 500:1 polarizer to generate p-polarized radiation (with respect to the plane of incidence). Au films (∼50 nm) were deposited onto BK-7 glass slides (Schott). These Au/BK-7 slides were placed glass-to-glass against one side of a BK-7 glass prism (Schott) with a drop of index matching fluid ($n = 1.515$) to ensure optical coupling between the two glass substrates. The reflected light from the prism was detected with a Si photodiode (Thorlabs, model DET 100). The output of the photodiode was sent to a lock-in amplifier (Stanford Research Systems, model 830) where it was referenced against the chopper frequency and the DC voltage recorded by a personal computer. The prism was mounted to a computer-controlled high-resolution rotation stage (Newport, model URM 100C). The resolution of the stage is 0.001°. In a typical SPR experiment, the step size was 0.01°.

Infrared Spectroscopy. Reflection−absorption infrared spectra (RAIRS) of a $C_{16}H_{33}Q^+$-3CNQ$^-$ LB monolayer on gold surface were measured on a Nicolet Magna-IR 560 ESP spectrometer with a liquid nitrogen cooled mercury cadmium telluride wide-band detector. The resolution was set to 2 cm^{-1}. The incident angle of the p-polarized light was 85° relative to the surface normal. A gold surface (150 nm thick), prepared in the same batch as the one with the organic monolayer on it, was cleaned by UV/ozone exposure for 80 s. For each spectrum, 1024 scans were averaged and ratioed to the clean gold surface.

The bulk IR spectra of $C_{16}H_{33}Q^+$-3CNQ$^-$ and reference compounds were recorded on a JASCO FT/IR spectrophotometer at resolution of 2 cm^{-1} by measuring the sample dispersed in a KBr pellet. For each spectrum, 32 scans were averaged, and the spectra were ratioed to a blank KBr pellet.

Raman Spectroscopy. Raman spectra of a microcrystalline sample of $C_{16}H_{33}Q^+$-3CNQ$^-$ were collected at the University of Parma, with a Renishaw System-1000 Raman microscope, using a magnifying objective of 50×. The radiation source of wavelength 568 nm was supplied by a Kr laser.

X-ray Photoelectron Spectroscopy. X-ray photoelectron spectra were acquired on a Kratos Analytical Axis 165 Scanning Auger/XPS spectrometer. Mg Kα X-ray photons (1253.6 eV) from a dual-anode source were used as exciting radiation for both angle-resolved and sputtering depth profile measurements. Monochromic Al Kα photons (1486.7 eV) were used for the

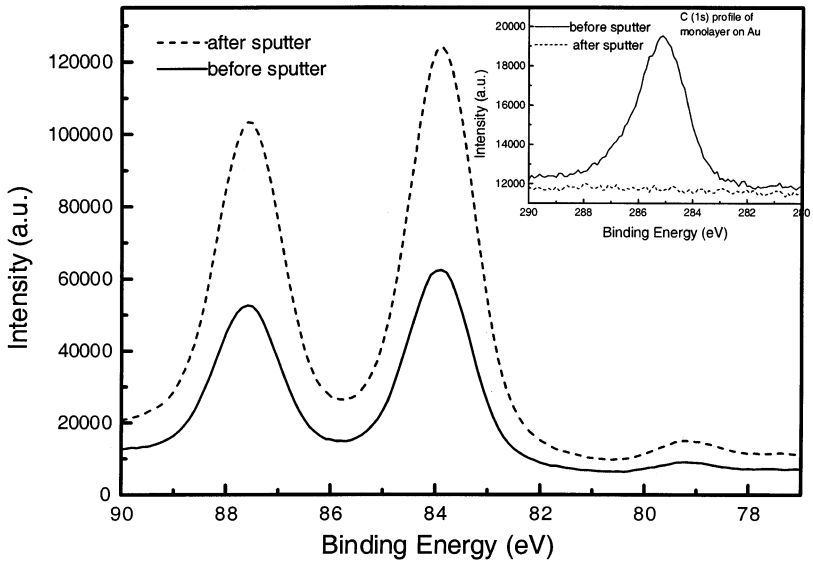

Figure 2. Au(4f) XPS sputtering depth profile of LB monolayer of $C_{16}H_{33}Q^+$-3CNQ$^-$ on gold film. The Au(4f) signal increases as the monolayer is removed. Inset: C(1s) signal before and after sputtering.

high-resolution measurements (20 scans). For angle-resolved XPS, an electrostatic lens was used. To avoid systematic errors in the measurements, the takeoff-angle (TOA), defined as the angle between the sample surface and the entrance to the energy analyzer, was varied in a random sequence of angles.

Simultaneous Electrochemical and Steady-State Absorption Measurements. Optical absorption spectra in the range 190−1100 nm were obtained on a Shimadzu UV-1601 UV−vis spectrophotometer. In a nitrogen-filled box, a 1×10^{-4} M solution of **1** in CH_2Cl_2, with 0.1 M NBu_4ClO_4 electrolyte added, was prepared and placed into a special spectroelectrochemical cell. This cell was divided into two chambers by a glass frit. The first chamber, fused to a quartz cuvette (10 mm path length) used for simultaneous bulk electrolysis and optical measurements, contains a Pt wire (working electrode) and an Ag wire (pseudo-reference electrode). Another Pt wire (counter electrode) was in the second chamber, separated from the first one by the glass frit. The cell was then placed into the UV−vis spectrometer, while the electrodes were connected to a BAS-100 B/W electrochemical analyzer. The bulk electrolysis of $C_{16}H_{33}Q^+$-3CNQ$^-$ was carried out in this three-electrode system at room temperature.

Contact Angle Goniometer. A Ramé−Hart contact angle goniometer (Naval Research Laboratory, Washington, DC) was used to measure, at room temperature and in air, the water contact angle on the clean gold surface and on the LB monolayer on gold. Under these conditions the contact angles were stable for at least a few minutes. For the measurement, 3 μL of water was dropped on the surface, followed by another 3 μL. The experimental error of this method is estimated to be ±3%, or ±1°.

Results and Discussion

Figure 1 shows the structure of $C_{16}H_{33}Q^+$-3CNQ$^-$ and related reference compounds. Figure 2 shows a high-resolution scan of the Au(4f) region before and after sputtering away the $C_{16}H_{33}Q^+$-3CNQ$^-$ monolayer on Au. The inset of Figure 2 shows the C(1s) region. The disappearance of the C(1s) photoelectron peak indicates complete removal of the carbon-containing species, i.e., the LB monolayer. The film thickness (for TOA = 90°) can be determined from $d = -\lambda \ln(I_d/I_0)$, where d is the LB monolayer thickness, λ is the mean free path

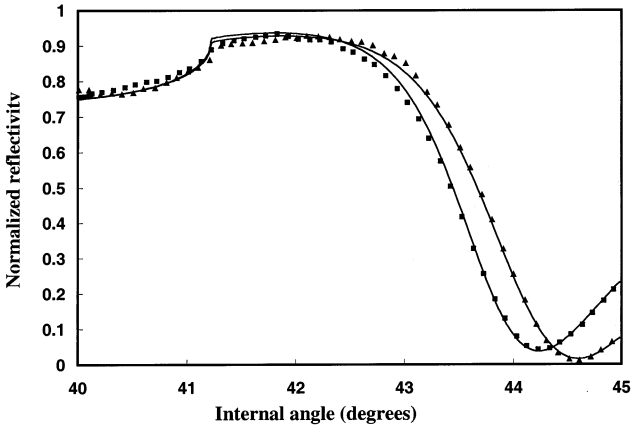

Figure 3. Normalized reflectivity versus angle of incidence for glass/Au (squares) and glass/Au/monolayer (triangles) at 632.8 nm. The line passing through the data is the "best" fit.

of the Au(4f) photoelectron, I_d is the Au(4f) intensity with the LB monolayer present, and I_0 is the Au(4f) intensity after sputtering. The mean free path of a Au(4f) photoelectron at 1253.6 − 88 = 1165.6 eV is calculated to be $\lambda = 32.5$ Å[16] and has been measured to be 34 Å.[17] Using the measured Au (4f) peak area and a value of $\lambda \sim 33$ Å, the thickness of the LB monolayer film becomes $d = 25.5 \pm 2$ Å.

The calculated length of the fully extended molecule is approximately 33 Å (CAChe),[12] so the film thickness measured by XPS implies that the molecules in the LB monolayer are not aligned perpendicularly on the gold surface, but at a tilt angle between the surface normal and molecular axis of $\cos^{-1}(25.5/33) = 39°$.

As an independent measure of the thickness of the LB film, surface plasmon resonance spectroscopy was performed on a clean Au surface before and after the deposition of $C_{16}H_{33}Q^+$-3CNQ$^-$. Figure 3 shows representative experimental and simulated SPR curves. The presence of the LB film increases the angle of minimum reflectivity and slightly decreases the absolute reflectivity at that angle. The simulated "best" fit curves were obtained by solving the Fresnel equations by Hansen's method.[18] The clean Au film parameters (~43 nm, $\epsilon' = -10.345 \pm 0.015$, $\epsilon'' = 1.37 \pm 0.06$) are consistent with published values of gold films prepared in a similar manner.[19] The LB film optical

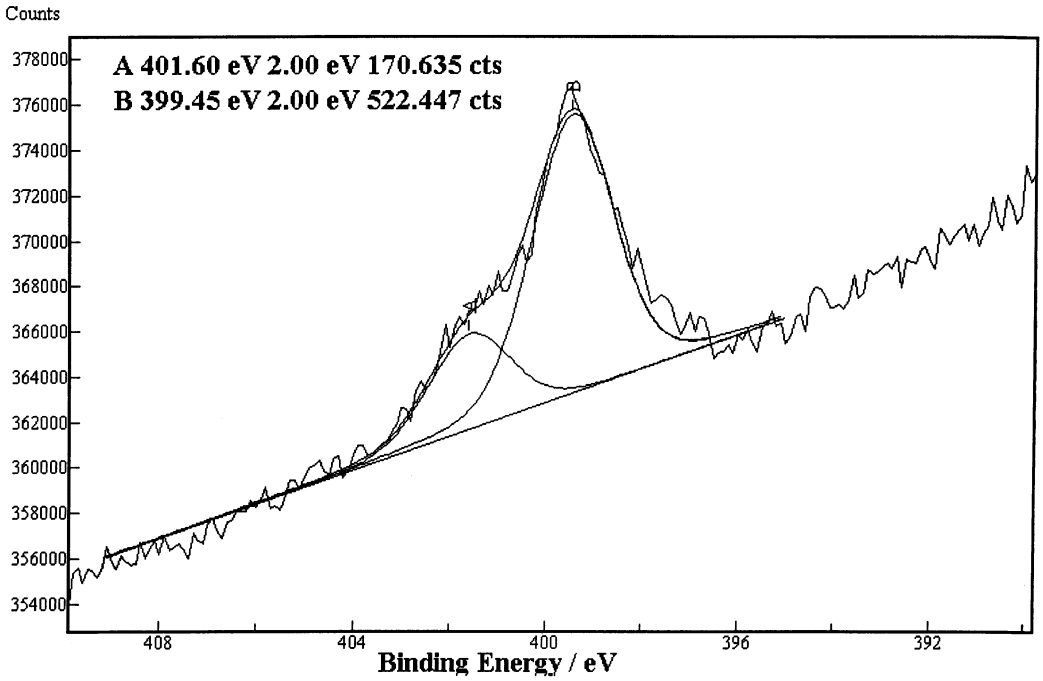

Figure 4. High-resolution N(1s) XPS of a $C_{16}H_{33}Q^+$-3CNQ$^-$ LB monolayer on Au.

TABLE 1: Summary of the Monolayer Film Thickness (Å) on Different Substrates Measured by Various Techniques

technique	SPR	XPS	ellipsometry	XRD
monolayer thickness(Å)	22.1 ± 1.4(Ag, 632.8 nm)[9] 20 ± 2(Au, 632.8 nm)	25.5 ± 2(Au)	21.5 ± 1.5(Ag, 670 nm)[9] 220 ± 0.2(Au, 750∼1000 nm)[5] 226 ± 2(Al, 632.8 nm)[8]	29.2(Au, glass)[5]

constants of $C_{16}H_{33}Q^+$-3CNQ$^-$ have been previously determined ($\epsilon' = 3.17$, $\epsilon'' = 0.3$)[9] and were used in this work as known parameters in the fit of the SPR curve after LB film deposition. The thickness of the LB film varied until a "best fit" of 20 ± 2 Å was obtained. Within experimental error, this result agrees quite well with a previously published value (∼22 Å) of the LB film thickness on Ag by SPR.[9]

We next discuss critically the film thickness determined by different methods (see Table 1). First, we consider what role may be played by adsorbates that physisorb to the LB films after they are removed from the desiccator. We suspect that volatile hydrocarbons and water vapor are the most likely adsorbates. These adsorbates would be present for measurements in air (ellipsometry, XRD, SPR), but under the high vacuum of the XPS chamber they may desorb slowly, through gaps in the LB monolayer. Second, we consider how the thickness is determined in the optical measurements (ellipsometry and SPR). For a monolayer of highly polar zwitterions, it may be a serious oversimplification to use a scalar value for the real and imaginary components of the dielectric tensor. Also, the use of the Fresnel equations for SPR and ellipsometry assumes that image dipoles or work function changes do not modify the dielectric tensor of the substrate (Au) at the interface. Thus, SPR and ellipsometry provide an indirect measurement of the thickness, because the data must be fit to an optical model. We suspect that the anomalously low thickness for the two optical measurements is due to the limitations in the optical models we used. Specifically, we ignored the image dipole layer that will exist in the gold film due to the large dipole of compound **1**. There is, indeed, evidence that even small dipolar layers on a gold films can be detected by ellipsometery. For example. Allara and co-wokers were able to detect the polarized Au−S bond in self-assembled monolayers formed from alkanethiols adsorbed to Au surfaces.[20]

For these reasons, the lower values of the film thickness (20 ± 2 Å by SPR), while agreeing with previous estimates by optical techniques, may be affected by the oversimplifications of the data analysis. The lone "high" value of 29 ± 2 Å was determined by X-ray diffraction.[5] This technique is sensitive to surface roughness and long-range order and may bias the measurement. XPS is the only method that measures the film under rigorously clean conditions (i.e., ultrahigh vacuum). For this reason XPS may provide the most reliable result, because weakly adsorbed contamination will get pumped away before the measurement.

We now discuss the X-ray photoelectron spectra. Figure 4 shows a high-resolution N(1s) core-level XPS spectrum of a LB monolayer on gold. The shoulder peak at a binding energy of 401.6 eV is associated[7] with the positively charged ammonium nitrogen (as in ammonium salts, e.g., $N^*H_4NO_3$ at 402.3 eV[21]). The main peak at 399.45 eV is due[11] to the nitrogens in cyano groups (C≡N).[22] The measured intensity ratio of the quinolinium nitrogen to the cyano nitrogens is 1:3, in excellent agreement with the molecular stoichiometry.

We next discuss the assignment of the most relevant vibrational modes of $C_{16}H_{33}Q^+$-3CNQ$^-$. Figure 5 shows the infrared and Raman spectra of $C_{16}H_{33}Q^+$-3CNQ$^-$ and the reference compounds $\mathbf{3}^+\mathbf{Br}^-$, **4**, $\mathbf{Li}^+\mathbf{2}^{\bullet-}$, and **2**. The peak assignments are summarized in Table 2. The C≡N vibrational modes are at 2222 cm^{-1} in neutral TCNQ (**2**), and close to 2183 cm^{-1} for fully ionic salts of TCNQ (the Li salt is somewhat anomalous).[23] In salts and complexes of TCNQ, the C≡N vibrational modes are susceptible to formal charge and to crystal field effects.[23] The effects of formal charge have been used to classify the ionicity of TCNQ salts,[24] but there also crystal field effects (i.e., band shifts due to the crystallographic inequivalence of C≡N groups in the same molecule and subtle distortions caused by crystallographic "packing"), and also the effects of

TABLE 2: Assignments of IR and Raman Bands (in cm^{-1}) and Relative Peak Heights of C≡N Stretch Bands (arbitrary units) for $C_{16}H_{33}Q^+$-3CNQ$^-$ (1) and Related Reference Compounds in Bulk Polycrystalline Powder Form (p) and for LB Monolayers of 1 on Either Au (m,Au) or on Al (m, Al)[a]

compound	benzenoid C−H out-of-plane bending mode	quinolinium C−H out-of-plane bending mode	vinyl ═C−H	C≡N stretch pos	C≡N stretch int.	CH_2 sym	CH_2 asym	CH_3 asym
1 (p)	826	754		2136 2176	0.5 1.00	2854	2920	not resolved
1 (p, Raman)	819			2139 2179 2217	0.58 1.00 4.08			
1 (m, Au)	840	780		2137 2177	2.04 1.00	2854	2920	2960
1 (m Al) [8]				2139 2175	2.14 1.00	2850	2920	not resolved
Li$^+$2$^{\bullet-}$ (p)	822			2190 2204	2190 2204			
2 (p)			860 bend 3050 stretch	2222	1.00			
3$^+$Br$^-$ (p)		759				2853	2920	not resolved
4		755		2174 2196	1.12 1.00	2850	2920	not resolved

[a] From reference 8.

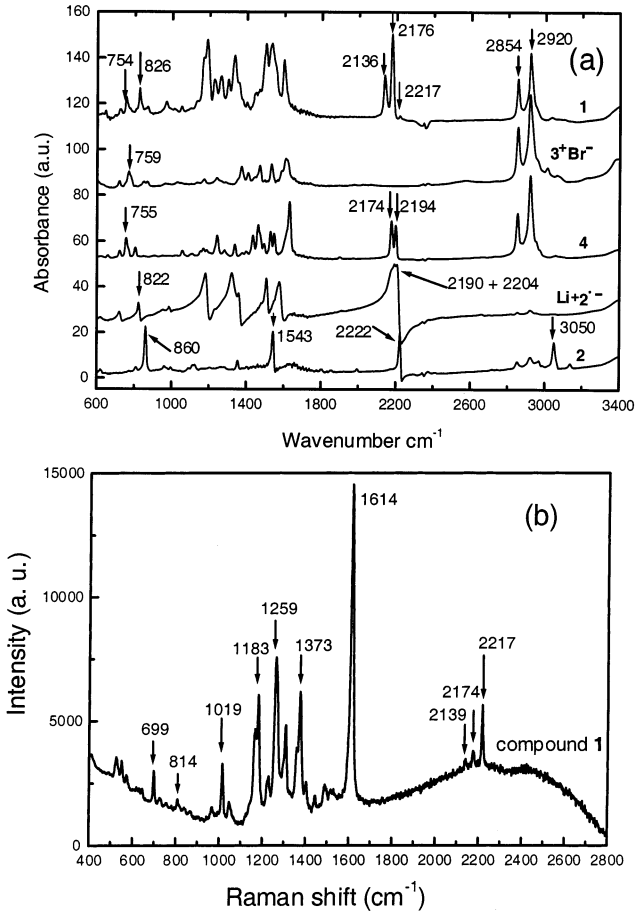

Figure 5. (a) Transmission infrared spectra of $C_{16}H_{33}Q^+$-3CNQ$^-$ and related compounds in KBr pellets. (b) Raman spectrum of $C_{16}H_{33}Q^+$-3CNQ$^-$ in bulk phase (polycrystalline).

pi-to-pi dimers of radical anions (or anions and neutral molecules) of TCNQ.[23] Such assignments have also been used for LB films of TCNQ-bearing compounds.[25] The C≡N bands may also be split in second order by mutual phase (two neighboring C≡N vibrations in phase with each other, or out of phase with each other). The electrochemistry of **1** reveals that it is not as potent a one-electron acceptor as TCNQ,[8] so the analogies between **1** and the ionized forms of TCNQ must be taken with a grain of salt. If one takes literally the valence-bond depiction of structure **1** in Figure 1, then molecule **1** has three C≡N groups, one formally "neutral" and the other two in the dicyanomethylene "tail" being formally "partially anionic".

In the IR spectrum of a polycrystalline sample of **1** (Figure 5(a)) there are three bands, two intense ones at 2136 cm^{-1} and 2176 cm^{-1} and a very weak one at 2217 cm^{-1}; in the Raman spectrum of a polycrystalline sample of **1** (Figure 5(b)) the intensities are reversed; there is an intense band at 2217 cm^{-1} and two weaker ones at 2174 cm^{-1} and 2139 cm^{-1}. In compound **4** there are two C≡N peaks in the IR, at 2194 cm^{-1} and at 2174 cm^{-1}. Clearly, the Raman peak at 2217 cm^{-1} for compound **1** should be assigned to the "neutral" C≡N stretch, while the "ionic bands" are split. The 2136 cm^{-1} peak is due to the in-phase stretch of the two "ionic" C≡N groups (with a transition dipole moment along the long axis of the molecule), and the higher-energy one at 2176 cm^{-1} is assigned to the higher-energy "out-of-phase" stretch of these same two groups (with the transition moment roughly along the line connecting the two C≡N groups). These latter assignments have been suggested by an AM1 analysis of these compounds. Similarly, the two peaks of compound **4** at 2174 cm^{-1} and 2194 cm^{-1} would be assigned to in-phase and out-of-phase C≡N stretches, but the molecule is more zwitterionic than the structure shown for **4** in Figure 1 would suggest.

The fingerprint region of $C_{16}H_{33}Q^+$-3CNQ$^-$ between 1000 and 1800 cm^{-1} contains several strong peaks due to in-plane modes in the aromatic rings (i.e., C═C and C−CN stretches). The peaks below 1000 cm^{-1} can be assigned by comparison with corresponding features in the reference compounds. The peak at 759 cm^{-1} for **3$^+$Br$^-$** is assigned to the C−H out-of-plane bending mode in the quinolinium ring.[26] The peak at 822 $cm^{-1}$for compound **Li$^+$2$^{\bullet-}$** is assigned to the benzene C−H out-of-plane bending mode.[27] The peak at 860 cm^{-1} for compound **2** is assigned to the aryl C−H out-of-plane bending mode.[28] By comparing the IR spectra of these compounds, one can deduce that the 754 cm^{-1}peak in **1** is associated with the quinolinium C−H out-of-plane bending mode, and the 826 cm^{-1} peak in **1** is assigned to the benzenoid C−H out-of-plane bending mode.

Figure 6 shows the RAIRS of a $C_{16}H_{33}Q^+$-3CNQ$^-$ LB monolayer on Au, and the peak frequencies are also summarized in Table 2. The peaks for the C−H and C≡N stretches in the monolayer film and bulk are nearly identical. In contrast, the peak frequencies for the benzenoid and the quinolinium out-

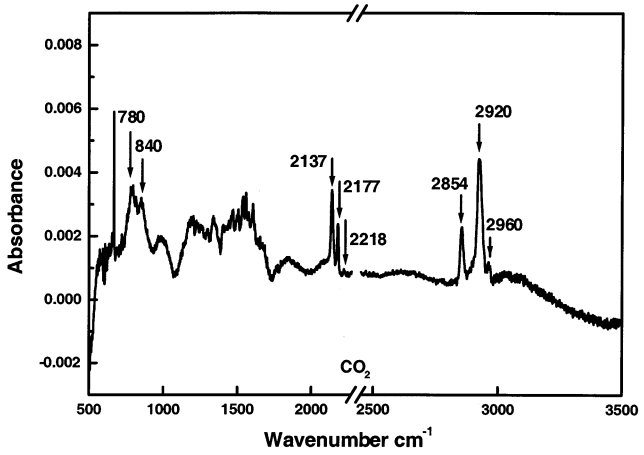

Figure 6. Reflection−absorption infrared spectrum of LB monolayer of $C_{16}H_{33}Q^+$-3CNQ$^-$ on Au(150 nm).

of-plane C−H stretches in the monolayer are 14 cm^{-1} and 26 cm^{-1} higher, respectively, than in the bulk-phase sample. The most obvious difference in the spectra of the monolayer film and bulk sample is the relative intensities of the peaks. In RAIRS, only molecular vibrations with a component of the transition dipole moment perpendicular to the surface are IR-active.[29] This indicates a preferred orientation of the molecules in the film. The intensities of the 2136 ± 1 cm^{-1} "in-phase" bands are enhanced for a monolayer of **1** on either Al[8] or Au, relative to the powder data, most likely because the long axis of the molecule is pointing out of the metal surface, while the 2176 cm^{-1} "out-of-phase" band is less intense for a monolayer on either Al[8] or Au, because the vector from one dicyanomethylene C≡N group to the other lies roughly in the metal plane.

The out-of-plane benzenoid and quinolinium C−H stretches and cyano stretches are more intense than the peaks in the fingerprint region. This observation suggests that the transition dipole moment of these modes is predominantly aligned along the surface normal. Furthermore, the intensity of the CH_3 asymmetric stretch mode at 2960 cm^{-1}, with respect to the bulk, indicates that the local C_{3v} symmetry axis of the CH_3 group is tilted with respect to the surface normal. The peak at 2920 cm^{-1} is due to the CH_2 asymmetric stretch mode, and is well known to indicate the degree of order in long-chain alkyl groups.[30] When the alkyl chains are well-packed and crystal-like, the CH_2 asymmetric stretch appears at 2920 cm^{-1}. When the chains are disordered and more liquid-like, the CH_2 asymmetric stretch mode moves to ∼2930 cm^{-1}. For example, in solution, or for a deliberately disordered monolayer of $C_{16}H_{33}Q^+$-3CNQ$^-$ on gold (obtained by transferring at a pressure of only 5 mN/m and at a fast film transfer speed), the CH_2 asymmetric stretch mode occurs at 2928 cm^{-1} (with a lower intensity relative to CH_3 asymmetric mode at 2962 cm^{-1}; data not shown).

Additional information about the molecular orientation is obtained by measurement of the water contact angle. The water contact angle on a clean gold film (newly evaporated gold film, cleaned by UV ozone for 80 s and immediately measured) is 40°, while the angle measured on a monolayer on gold is 92°. The contact angle for a fresh and clean surface should be close to 0°, but it is well known that clean gold surfaces readily accumulate a thin layer of organic contamination.[31] The results indicate that the hydrophobic hexadecyl aliphatic group of $C_{16}H_{33}Q^+$-3CNQ$^-$ is pointing away from the surface (correspondingly, the hydrophilic tricyanoquinodimethanide end should be closer to the Au surface).

Figure 7 shows angle-resolved XPS measurements on a $C_{16}H_{33}Q^+$-3CNQ$^-$ LB monolayer on Au. With decreasing takeoff-angle (TOA), there is a change in the intensity ratio between the quinolinium nitrogen and the three cyano nitrogens, from 1:3 at TOA = 90° to 1:2 at TOA = 30°. This suggests that the quinolinium nitrogen is further away from the Au surface and its photoelectrons are less attenuated, compared to the cyano nitrogens. Therefore, the quinolinium nitrogen must be above the three cyano groups in the monolayer of $C_{16}H_{33}Q^+$-3CNQ$^-$ on Au. We believe that the hexadecyl chain is hydrophobic enough to force molecules into a parallel alignment at the air−water interface. A monolayer of $C_{16}H_{33}Q^+$-3CNQ$^-$ can be transferred onto the Au substrate. In contrast, the intensity ratio of the ammonium nitrogen to the cyano nitrogen in an LB monolayer of $(C_{10}H_{21})_2N^+$-3CNQ$^-$ (structure **5** in Figure 1) does not show significant variation with the decreasing TOA,[32] which indicates that the decyl chain is not hydrophobic enough to force all molecules into a parallel alignment.[9,32]

Spectroelectrochemical absorption experiments on $C_{16}H_{33}Q^+$-3CNQ$^-$ and its related reference compounds can help to understand the charge-separated ground state.[13,14] The bulk electrolysis potentials were chosen slightly above the redox peak potentials of the cyclic voltammogram of $C_{16}H_{33}Q^+$-3CNQ$^-$ (−0.545 V vs SCE for reduction and 0.49 V vs SCE for oxidation).[8] Figure 8 shows the UV−vis spectrum of $C_{16}H_{33}Q^+$-3CNQ$^-$ in CH_2Cl_2 as a function of time elapsed during electrolytic reduction. The peak at 810 nm, due to intervalence charge transfer (IVT),[7] decreases with increasing reduction time, which indicates the disappearance of the conjugation cross the donor and acceptor by adding an electron to the donor. The species **1**$^{\bullet-}$ in Figure 1 is a possible structure for the radical anion of **1**,[8] in which the conjugation does not cross the whole molecule. A new peak at 435 nm rises with increasing reduction time. This band most likely results from the quinoline moiety in the radical anion **1**$^{\bullet-}$.

An obvious isosbestic point is observed at 531 nm, indicating that the disappearing IVT band at 810 nm is associated with the new peak rising at 435 nm. The presence of an isosbestic point is a strong argument in favor of the existence of two optically absorbing species. To verify that the compound does not decompose, a reoxidation of this radical was carried out (Figure 8, thicker solid line). The 810 nm band recovers as reoxidation progresses. Because the band at 810 nm can only result from IVT between the donor and acceptor moieties, the recovery of the peak at 810 nm indicates that the molecules do not decompose under the initial electrolytic reduction. The salt **3**$^+$**Br**$^-$ is a reference for the donor moiety in $C_{16}H_{33}Q^+$-3CNQ$^-$. Figure 9 shows the absorption of **3**$^+$**Br**$^-$ at different electrochemical reduction times. A new peak again appears with increasing reduction time, but at 380 nm. However, for this electrochemically generated species, there is a 50 nm shift between the absorption maximum of **3**$^\bullet$ (i.e., the radical generated from **3**$^+$ **Br**$^-$ by reduction) and the maximum for **1**$^{\bullet-}$ (i.e., the radical anion generated by reduction of $C_{16}H_{33}Q^+$-3CNQ$^-$, **1**). We assume that this shift of 50 nm results from the longer conjugation due to the extra C=C on the donor moiety of radical anion **1**$^{\bullet-}$. Therefore, molecule **4** is a reasonable reference compound for the donor moiety in radical anion **1**$^{\bullet-}$. The absorption band of **4** appears as a doublet at 434 and 412 nm (inset of Figure 8), which is in agreement with the new peak at 435 nm for radical anion **1**$^{\bullet-}$.

The UV−vis absorption of $C_{16}H_{33}Q^+$-3CNQ$^-$ was also measured during oxidation. Figure 10 shows the absorbance of

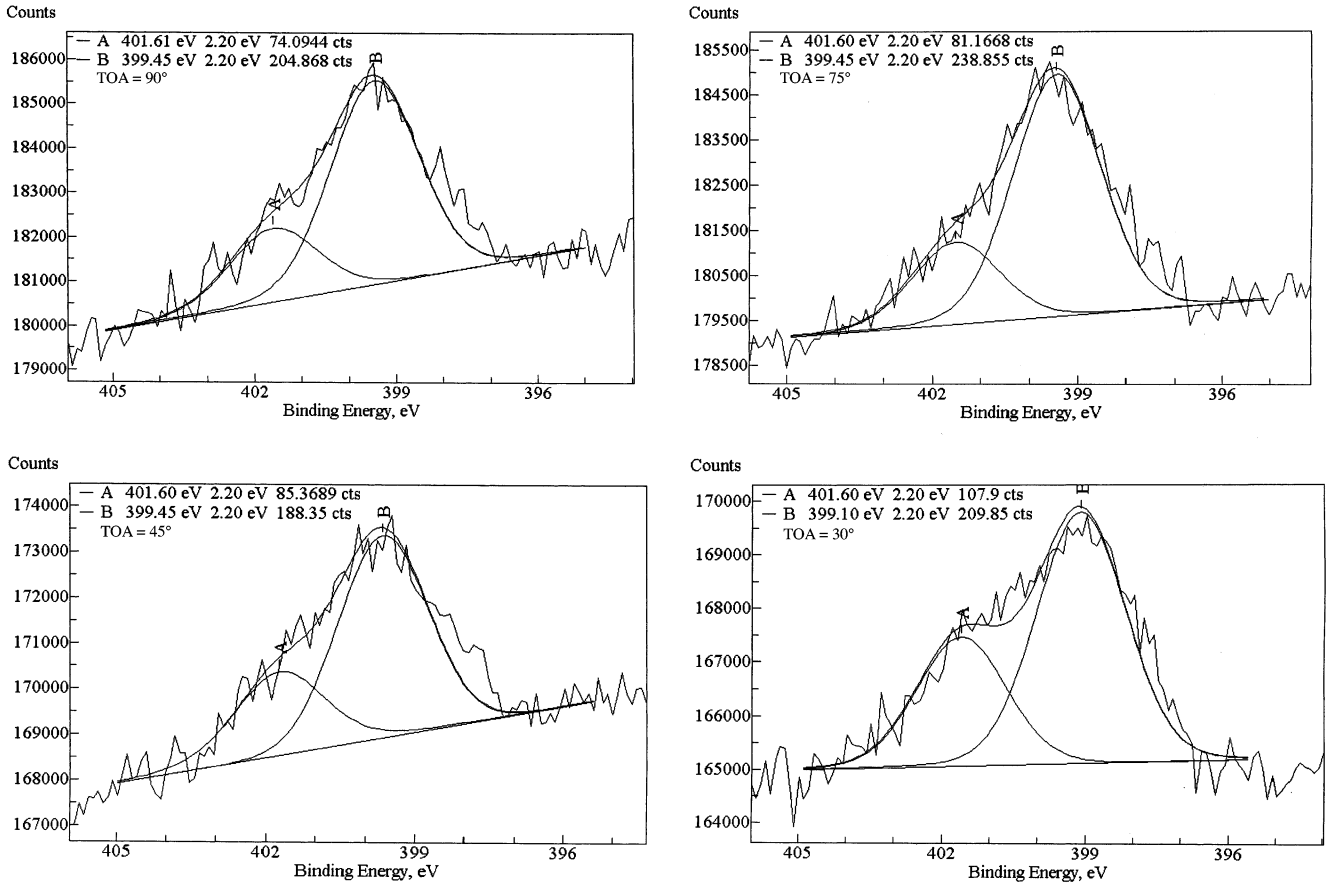

Figure 7. N(1s) angle-resolved XPS of $C_{16}H_{33}Q^{+}$-3CNQ^{-} LB monolayer on Au.

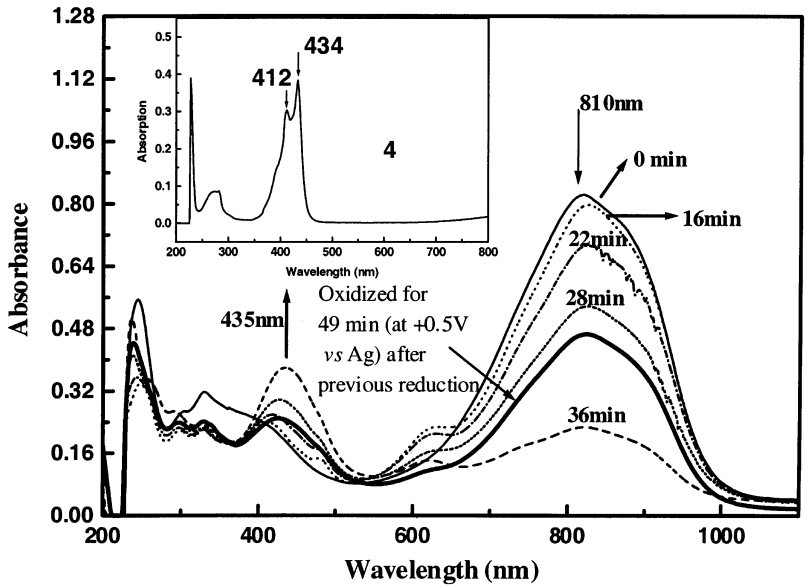

Figure 8. UV−vis absorption of 1.0×10^{-4} M $C_{16}H_{33}Q^{+}$-3CNQ^{-} in CH_2Cl_2 electrochemically reduced at −0.6 V vs Ag for various times (0 min [thin solid line], 16 min [.....], 22 min [·-·-·-·], 28 min [- - -], 36 min [– – –]), and then oxidized at 0.5 V vs.Ag for 49 min [thicker solid line]. Inset: Absorption of compound **4**.

$C_{16}H_{33}Q^{+}$-3CNQ^{-} for different durations of electrolytic oxidation. Again, the peak at 810 nm due to intervalence charge transfer decreases with the increasing oxidation time, which indicates the disappearance of the electronic mixing of states between the electron donor moiety and the electron acceptor moiety. The species $\mathbf{1}^{\bullet+}$ is a possible valence structure for the radical cation of **1**. The peak at 328 nm rises with increasing oxidation time. The donor part of $\mathbf{1}^{\bullet+}$ resembles that of reference compound $\mathbf{3}^{+}\mathbf{Br}^{-}$, which shows an absorption band at 318 nm, in agreement with the rising peak at 328 nm of $\mathbf{1}^{\bullet+}$. The isosbestic point appears at 393 nm. Again, to verify that the compound **1** does not decompose, a rereduction was followed (absorption after 17 min rereduction was shown in Figure 10). The 810 nm band recovers during further reduction. The recovered peak at 810 nm indicates that the molecules do not decompose under oxidation if this is carried out slowly enough (at a scan rate of 20 mV/s, the oxidation peak is not electrochemically reversible).[8]

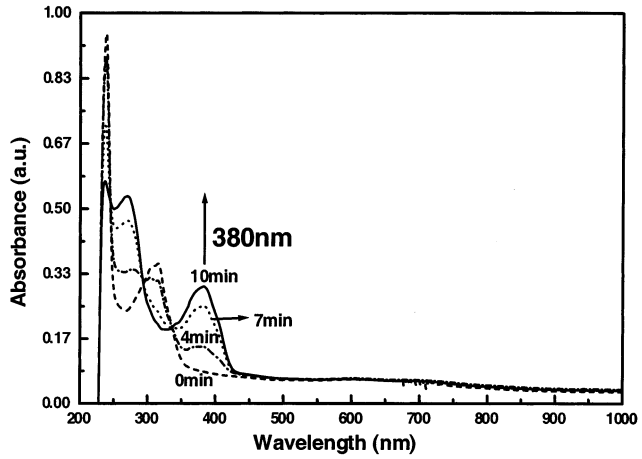

Figure 9. UV−vis absorption of 1.0×10^{-4} M $\mathbf{3}^+\mathbf{Br}^-$ in CH_2Cl_2 electrochemically reduced at −0.5 V vs Ag for different times (0 min [- - - -], 4 min [•-•-], 7 min [....], 10 min [solid line]).

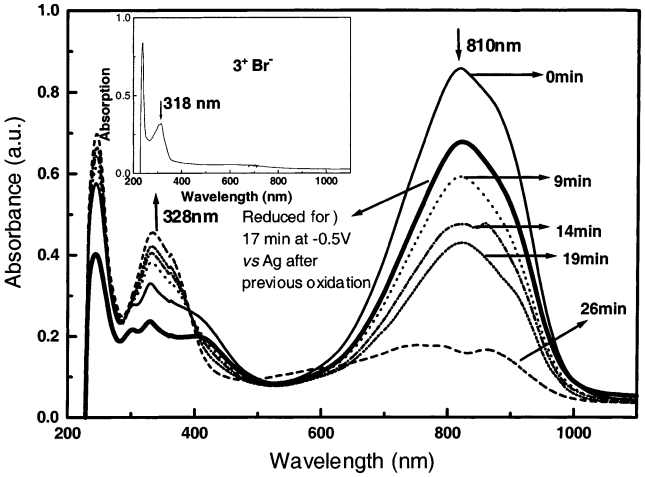

Figure 10. UV−vis absorption of 1.0×10^{-4} M $C_{16}H_{33}Q^+$-3CNQ$^-$ in CH_2Cl_2 electrochemically oxidized at +0.5 V vs Ag for different times, and then reduced (at −0.5 V) for 17 min (thicker solid line). Inset: absorption of compound $\mathbf{3}^+\mathbf{Br}^-$.

Conclusions

It was shown that the molecule $C_{16}H_{33}Q^+$-3CNQ$^-$ is a ground-state zwitterion and that it orders in a parallel polar arrangement as an LB monolayer on a Au surface. The film thickness by SPR and ellipsometry is measured to be 22 Å, which is slightly less than the value of 25.5 Å obtained by XPS. The molecules are probably tilted about 40° from the surface normal, and the ground-state dipoles are oriented parallel to each other. The monolayer lies on the Au surface with the two terminal cyano groups closest to the Au, and the alkyl chains ordered and facing away from the Au. The infrared spectral features of an LB monolayer of $C_{16}H_{33}Q^+$-3CNQ$^-$ can be assigned to specific vibrational modes by using model compounds. The oxidation and reduction of $C_{16}H_{33}Q^+$-3CNQ$^-$ is accompanied by the disappearance of the IVT band, which is recovered when the electrolysis is carried out in the reverse direction.

Acknowledgment. We are grateful to Dr. Earl Ada for stimulating discussions and technical support, and to the National Science Foundation (NSF DMR-0095235) for financial support.

References and Notes

(1) Schön, J. H.; Meng, H.; Bao, Z. *Nature* **2001**, *413*, 713.

(2) Cui, X. D.; Primak, A.; Zarate, X.; Tomfohr, J.; Sankey, O. F.; Moore, A. L.; Moore, T. A.; Gust, D.; Harris, G.; Lindsay, S. M. *Science* **2001**, *294*, 571.

(3) Metzger, R. M. *Acc. Chem. Res.* **1999**, *32*, 950.

(4) Xu, T.; Peterson, I. R.; Lakshmikantham M. V.; Metzger, R. M. *Angew. Chem., Int. Ed. Engl.* **2001**, *40*, 1749.

(5) Metzger, R. M.; Xu, T.; Peterson, I. R. *J. Phys. Chem. B* **2001**, *105*, 7280.

(6) Krzeminski, C.; Delerue, C.; Allan, G.; Vuillaume, D.; Metzger, R. M. *Phys. Rev. B* **2001**, *64*, #085405.

(7) Baldwin, J. W.; Chen, B.; Street, S. C.; Konovalov, V. V.; Sakurai, H.; Hughes, T. V.; Simpson, C. S.; Lakshmikantham, M. V.; Cava, M. P.; Kispert, L. D.; Metzger, R. M. *J. Phys. Chem. B* **1999**, *103*, 4269.

(8) Metzger, R. M.; Chen, B.; Höpfner, U.; Lakshmikantham, M. V.; Vuillaume, D.; Kawai, T.; Wu, X.; Tachibana, H.; Hughes, T. V.; Sakurai, H.; Baldwin, J. W.; Hosch, C.; Cava, M. P.; Brehmer, L.; Ashwell, G. J. *J. Am. Chem. Soc.* **1997**, *119*, 10455.

(9) Ashwell, G. J.; Jefferies, G.; Dawnay, E.; Kuczynski, A.; Lynch, D.; Yu, G.; Bucknall, D. *J. Mater. Chem.* **1995**, *5*, 975.

(10) Aviram, A.; Ratner, M. A. *Chem. Phys. Lett.* **1974**, *29*, 227.

(11) Yaliraki, S. N.; Kemp, M.; Ratner, M. A. *J. Am. Chem. Soc.* **1999**, *212*, 3428.

(12) Hall, L. E.; Reimers, J. R.; Hush, N. S.; Silverbrook, K. *J. Chem. Phys.* **2000**, *112*, 1510.

(13) Hayes, R. T.; Wasielewski, M. R.; Gosztola, D. *J. Am. Chem. Soc.* **2000**, *122*, 5563.

(14) Greenfield, S. R.; Svec, W. A.; Gosztola, D.; Wasielewski, M. R. *J. Am. Chem. Soc.* **1996**, *118*, 6767.

(15) Knoll, W. *Annu. Rev. Phys. Chem.* **1998**, *49*, 569.

(16) Inelastic Mean Free Path Database Software, National Institute of Standards and Technology Database, U.S. Department of Commerce.

(17) Bain, C. D.; Whitesides, G. M. *J. Phys. Chem.* **1989**, *93*, 1670.

(18) Hansen, W. N. *J. Opt. Soc. Am.* **1968**, *58*, 380.

(19) Georgiadis, R.; Peterlinz, K. P.; Peterson, A. W. *J. Am. Chem. Soc.* **2000**, *122*, 3166.

(20) Shi, J.; Hong, D.; Parikh, A. N.; Collins, R. W.; Allara, D. L. *Chem. Phys. Lett.* **1995**, *246*, 90−94.

(21) Burger, K.; Tschismarov, F.; Ebel, H. *J. Electron Spectrosc. Relat. Phenom.* **1977**, *10*, 461.

(22) Vannerberg, N. G. *Chem. Scr.* **1976**, *9*, 122.

(23) Kunkeler, P. J.; van Koningsbruggen, P. J.; Cornelissen, J. P.; van der Horst, A. N.; van der Kraan, A. M.; Spek, A. L.; Haasnoot, J. G.; Reedijk, J. *J. Am. Chem. Soc.* **1996**, *118*, 2190.

(24) Chappel, J. S.; Bloch, A. N.; Bryden, W. A.; Maxfield, M.; Poehler, T. O.; Cowan, D. O. *J. Am. Chem. Soc.* **1981**, *103*, 2442−2443.

(25) Terashita, S.; Ozaki, Y.; Yageta, H.; Kudo, K.; Iriyama, K. *Langmuir* **1994**, *10*, 1811.

(26) Melby, L. R.; Harder, R. J.; Hertler, W. R.; Mahler, W.; Benson, R. E.; Mochel, W. E. *J. Am. Chem. Soc.* **1962**, *84*, 3374.

(27) Lunelli, B.; Pecile, C. *J. Chem. Phys.* **1970**, *52*, 2375.

(28) Takenaka, T. *Spectrochim. Acta* **1971**, *27A*, 1735.

(29) Greenler, R. G. *J. Chem. Phys.* **1966**, *44*, 310.

(30) Sapper, H.; Cameron, D. G.; Mantsch, H. H. *Can. J. Chem.* **1981**, *59*, 2543.

(31) Bain, C. D.; Troughton, E. B.; Tao, Y.-T.; Evall, J.; Whitesides, G. M.; Nuzzo, R. G. *J. Am. Chem. Soc.* **1989**, *111*, 321.

(32) Xu, T.; Morris, T. A.; Szulczewski, G. J.; Metzger, R. M. *J. Mater. Chem.*, in press.